Control limit on quantum state preparation under decoherence

Kohei Kobayashi and Naoki Yamamoto

Phys. Rev. A **99**, 052347 — Published 28 May 2019

DOI: 10.1103/PhysRevA.99.052347

Control limit on quantum state preparation under decoherence

Kohei Kobayashi and Naoki Yamamoto
Keio University, Department of Applied Physics and Physico-Informatics,
Hiyoshi 3-14-1, Kohoku, Yokohama, 223-8522, Japan
(Dated: May 6, 2019)

Quantum information technologies require careful control for generating and preserving a desired target quantum state. The biggest practical obstacle is, of course, decoherence. Therefore, the reachability analysis, which in our scenario aims to estimate the distance between the controlled state under decoherence and the target state, is of great importance to evaluate the realistic performance of those technologies. This paper presents a lower bound of the fidelity-based distance for a general open Markovian quantum system driven by decoherence process and several type of control including feedback. The lower bound is straightforward to calculate and can be used as a guide for choosing the target state, as demonstrated in some examples. Moreover, the lower bound is applied to derive a theoretical limit in some quantum metrology problems based on a large-size atomic ensemble under control and decoherence.

I. INTRODUCTION

It is no doubt that a carefully-designed control plays a key role in quantum information science. The open-loop (i.e., non-feedback) control theory [1–8] offers several powerful means, e.g., for implementing an efficient quantum gate operation. The measurement-based feedback (MBF) [9–16] and reservoir engineering including coherent feedback [17–23] are also well-established methodologies that can be used for generating and protecting a desired quantum state. Remarkably, many notable experiments realizing those control techniques have been demonstrated [24–29], which at the same time show that the actual control performance in the presence of decoherence is sometimes far away from the ideal one. Therefore the *reachability analysis* is essential to evaluate the practical effectiveness of those control methods; that is, it is important to quantify how close the controlled quantum state can be steered to or preserved at around a target state under decoherence. Note that the reachability characteristic determines a lower bound of the time required for performing a desired state transformation via control [30].

The reachability analysis found in the literature are usually based on simulations, which numerically investigate how much the ideal state control is disturbed by decoherence; for example, generation of a nano-resonator superposition state via open-loop control [5, 6], an optical Fock state via MBF [11, 14], and an opto-mechanical cat state via reservoir engineering [20, 23]. The optimal control method is also often used, which numerically designs a time-dependent control input for steering the state closest to the target under decoherence [3, 31]. However, these computational approaches do not give us a deep insight into basic questions for quantum engineering, e.g., what state should be targeted, what is the limit of realistic state preparation, and what is the desired structure of open quantum systems under given decoherence. A few exceptions are found for specific type of open-loop control [32] and MBF [33, 34], but there has been no unified approach. Also the controllability property, which is a stronger notion than the reachability, can be analytically investigated using the Lie algebra [35–40]; but they do not quantify the distance to the target and thus do not answer the above questions.

The main contribution of this paper is to present a limit for reachability, applicable for a general open Markovian quantum system driven by decoherence process and several type of controls including the open-loop and MBF controls and reservoir engineering; more precisely, we give a lower bound of the fidelity-based distance between a given target state and the controlled state under decoherence. This lower bound is straightforward to calculate, without solving any equation. Also thanks to its generic form, the lower bound gives a characterization of target states that are largely affected by the decoherence, and thereby provides us a useful guide for choosing the target, as demonstrated in some examples. Moreover, as "a deep insight into quantum engineering", the lower bound is used to derive a theoretical limit in quantum metrology; for a typical large-size atomic ensemble under control and decoherence, the fidelity to the target (the GHZ state or a highly entangled Dicke state) must be less than 0.875, without respect to the control strategy.

II. THE CONTROL LIMIT

A. Controlled quantum dynamics

We begin with a simplified setting of open-loop control and reservoir engineering; the quantum state $\bar{\rho}_t$ obeys the Markovian master equation

$$\frac{d\bar{\rho}_t}{dt} = -i[u_t H, \bar{\rho}_t] + \mathcal{D}[L]\bar{\rho}_t + \mathcal{D}[M]\bar{\rho}_t, \tag{1}$$

where H is a system Hamiltonian. L and M are Lindblad operators, and hence $\mathcal{D}[A]\bar{\rho} = A\bar{\rho}A^\dagger - A^\dagger A\bar{\rho}/2 - \bar{\rho}A^\dagger A/2$. Here L represents the uncontrollable "L"indblad operator corresponding to the decoherence, while M can be engineered; in particular in the MBF setting M represents the probe for "M"easurement. The standard open-loop control problem is to design a time-dependent sequence u_t that steers $\bar{\rho}_t$ toward a target state, under $M = 0$. Also the standard reservoir engineering approach aims to design M, with constant u_t, so that $\bar{\rho}_t$ autonomously converges to a target.

The MBF control setting can also be included in the theory. In this case the quantum state ρ_t conditioned on the measurement record y_t obeys the following stochastic master equation (SME) [41–43]:

$$d\rho_t = -i[u_t H, \rho_t]dt + \mathcal{D}[L]\rho_t dt + \mathcal{D}[M]\rho_t dt + \mathcal{H}[M]\rho_t dW_t, \tag{2}$$

where $dW_t = dy_t - \mathrm{Tr}[(M + M^\dagger)\rho_t]dt$ is the Wiener increment representing the innovation process based on y_t, and $\mathcal{H}[A]\rho = A\rho + \rho A^\dagger - \mathrm{Tr}[(A + A^\dagger)\rho]\rho$. The goal of MBF is to design the control signal u_t as a function of ρ_t, to achieve a certain goal. In particular, if $L = 0$ and $M = M^\dagger$, there are several type of MBF controls that selectively steer the state to an arbitrary eigenstate of M. In this paper, we focus on the unconditional state $\bar{\rho}_t = \mathbb{E}(\rho_t)$, which is the ensemble average of ρ_t over all the measurement results. Then due to $\mathbb{E}(W_t) = 0$, Eq. (2) leads to the following master equation:

$$\frac{d\bar{\rho}_t}{dt} = -i[H, \mathbb{E}(u_t\rho_t)] + \mathcal{D}[L]\bar{\rho}_t + \mathcal{D}[M]\bar{\rho}_t. \tag{3}$$

Note that now u_t is a function of ρ_t, and thus Eq. (3) is not a linear equation with respect to $\bar{\rho}_t$. In the open-loop control or reservoir engineering setting, meaning that u_t is independent of ρ_t, then Eq. (3) is reduced to the linear equation (1) due to $\mathbb{E}(u_t\rho_t) = u_t\bar{\rho}_t$.

B. Main result

The control goal is to minimize the following cost function:

$$J_t = 1 - \langle\psi|\bar{\rho}_t|\psi\rangle, \tag{4}$$

where $|\psi\rangle$ is the target pure state and $\bar{\rho}_t$ is the controlled state obeying Eq. (1) or (3); hence, J_t represents the fidelity-based distance of $\bar{\rho}_t$ from the target. Under the presence of decoherence term $\mathcal{D}[L]$, in general it is impossible to deterministically achieve $J_t = 0$ at some time t. The main result of this paper is to provide a lower bound of the cost in an explicit form as follows. The proof is given in Appendix A.

Theorem: The cost (4) has the following lower bound at the steady state:

$$J_\infty \geq J_*(|\psi\rangle) = \left(\frac{\mathcal{E}}{\mathcal{A} + \mathcal{U}}\right)^2, \tag{5}$$

where ($\||\psi\rangle\|^2 = \langle\psi|\psi\rangle$ is the Euclidean norm)

$$\begin{aligned}\mathcal{A} &= \sqrt{2}\big(\|L^\dagger|\psi\rangle\|^2 + \|L^\dagger L|\psi\rangle\| \\ &\qquad + \|M^\dagger|\psi\rangle\|^2 + \|M^\dagger M|\psi\rangle\|\big), \\ \mathcal{U} &= 2\bar{u}\sqrt{\langle\psi|H^2|\psi\rangle - \langle\psi|H|\psi\rangle^2}, \quad \bar{u} = \max\{|u_t|\}, \\ \mathcal{E} &= \|L|\psi\rangle\|^2 - |\langle\psi|L|\psi\rangle|^2 + \|M|\psi\rangle\|^2 - |\langle\psi|M|\psi\rangle|^2.\end{aligned}$$

Moreover, if $J_{t_0} \geq J_*$ for an initial state $\bar{\rho}_{t_0}$, then $J_t \geq J_*$ holds for all $t \in [t_0, \infty)$.

That is, J_* gives a limit on how close the controlled quantum state can be steered to or preserved at around a target state under decoherence. Below we list some notable general features of J_*.

(i) The theorem is applicable to a general Markovian open quantum systems driven by several type of control including the MBF and reservoir engineering.

(ii) The result can be extended to the case where the system is subjected to multiple environment channels, measurement probes, and control Hamiltonians, as long as the dynamical equation can be validly described as an extension of Eq. (1) or (2); see Appendix B.

(iii) J_* is directly computable, once the system operators and the target state $|\psi\rangle$ are specified; it is not necessary to solve any equation.

(iv) J_* is a monotonically decreasing function of the control magnitude $\bar{u}$.

(v) If $|\psi\rangle$ moves away from the eigenstates of L and M, then J_* becomes bigger. Conversely, $J_* = 0$ if and only if $|\psi\rangle$ is identical to a common eigenvector of L and M.

Importantly, J_* can be used to characterize a target state that is possibly easy to approach by some control, under a given decoherence. That is, a state $|\psi\rangle$ with relatively small value of J_* might be a good candidate as the target, although in general J_* is not achievable. Conversely, we can safely say that the state $|\psi\rangle$ with relatively large value of J_* should not be assigned as the target. In what follows we study some typical control problems, with special attention to this point.

III. EXAMPLES

A. Qubit

The first example is a qubit such as a two-level atom, consisting of $|e\rangle = [1, 0]^\top$ and $|g\rangle = [0, 1]^\top$. Let the target be a pure qubit state

$$|\psi\rangle = [\cos\theta,\ e^{i\varphi}\sin\theta]^\top,\ (0 \leq \theta < \pi/2,\ 0 \leq \varphi < 2\pi). \tag{6}$$

Here we consider the following operators:

$$H = \sigma_y,\ M = \sqrt{\kappa}\sigma_z,\ L = \sqrt{\gamma}\sigma_-,$$

where $\sigma_y = i(|g\rangle\langle e| - |e\rangle\langle g|)$, $\sigma_z = |e\rangle\langle e| - |g\rangle\langle g|$, and $\sigma_- = |g\rangle\langle e|$. This is a typical MBF control setup [10, 25–27]; M represents the engineered dispersive coupling between the qubit and the probe, which enables us to continuously monitor the qubit state by measuring the probe output and thereby perform a MBF control via the Hamiltonian $u_t H$. Ideally (i.e., if $\gamma = 0$), this MBF realizes deterministic and selective steering of the qubit state to $|e\rangle$ or $|g\rangle$. However in practice this perfect control is not allowed due to decoherence $L = \sqrt{\gamma}\sigma_-$, i.e., energy decay from $|e\rangle$ to $|g\rangle$ for a two-level atom. In this setup, the lower bound J_* is calculated as

$$J_* = \frac{1}{2}\left[\frac{\kappa \sin^2 2\theta + \gamma \cos^4\theta}{2\kappa + \gamma(\sin^2\theta + \cos\theta) + \bar{u}\sqrt{2 - 2\sin^2 2\theta \sin^2\varphi}}\right]^2.$$

A detailed derivation of this expression (and that of J_* in the other examples) is provided in Appendix D.

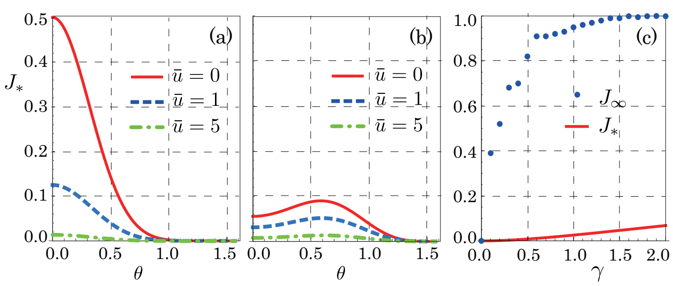

FIG. 1: The lower bound J_* as a function of θ for (a) $\kappa = 0$ and (b) $\kappa = 1$, in unit of $\gamma = 1$. (c) J_* and J_∞ with u_t a special type of MBF control input, for the case $|\psi\rangle = |e\rangle$ and $(\kappa, \bar{u}) = (1, 1)$.

First, we set $\kappa = 0$; this is the case where the system obeys the master equation $d\bar{\rho}_t/dt = -i[u_t\sigma_y, \bar{\rho}_t] + \mathcal{D}[\sqrt{\gamma}\sigma_-]\bar{\rho}_t$ driven by the open-loop control input u_t satisfying $|u_t| \le \bar{u}$ [8, 18, 35, 40]. Figure 1(a) shows the above lower bound J_* in unit of $\gamma = 1$, for the target satisfying $\varphi = 0$. Clearly, J_* takes the maximum at $|\psi\rangle = |e\rangle$ and zero at $|\psi\rangle = |g\rangle$ for each $\bar{u}$, implying that $|e\rangle$ is the most difficult state to approach, while $|g\rangle$ could be stabilized exactly; in fact these implications are true, as can be analytically verified by solving the above master equation. On the other hand if $\kappa = 1$, as depicted in Fig. 1(b), J_* at around $\theta = 0$ remarkably decreases compared to the case $\kappa = 0$. This is reasonable because the dispersive interaction represented by $M = \sqrt{\kappa}\sigma_z$ enables us to perform a MBF control that deterministically stabilizes $|e\rangle$ if $\gamma = 0$. As a consequence, J_* takes the maximum at around $\theta = 0.6$, meaning that a superposition is the most difficult state to reach.

It is also worth comparing J_* to the actual distance J_∞ achieved by a special type of MBF. We particularly take the method proposed in [15] and compute J_∞ by averaging 300 sample points of conditional state ρ_t at steady state, for the case $|\psi\rangle = |e\rangle$ and $(\kappa, \bar{u}) = (1, 1)$ with several value of γ; see Appendix C for the details. Figure 1(c) shows that the gap between J_* and J_∞ is large and hence J_* is not a tight lower bound in this case; but one could take another control strategy to reduce the gap and eventually prepare a state close to $|e\rangle$.

B. Two-qubits

Here we study a two-qubits system under decoherence. First let us focus on the following Bell states, which are of particular use in the scenario of quantum information science [44]:

$$|\Phi^\pm\rangle = \frac{1}{\sqrt{2}}\left(|g, g\rangle \pm |e, e\rangle\right), \ |\Psi^\pm\rangle = \frac{1}{\sqrt{2}}\left(|g, e\rangle \pm |e, g\rangle\right).$$

The question here is which Bell state is the best accessible one by any open-loop control (hence assume $M = 0$) [8]; as seen in the qubit case, the lower bound J_* gives us a rough estimate of the answer. We particularly consider the collective decay process modeled by $L = \sqrt{\gamma}(\sigma_- \otimes I + I \otimes \sigma_-)$. Then, for the case $|\Phi^+\rangle$, we have $\mathcal{E} = \|L|\Phi^+\rangle\|^2 - |\langle\Phi^+|L|\Phi^+\rangle|^2 = \gamma$ and $\mathcal{A} = \sqrt{2}(\|L^\dagger|\Phi^+\rangle\|^2 + \|L^\dagger L|\Phi^+\rangle\|) = (2+\sqrt{2})\gamma$. Hence, together with the other Bell states, the lower bounds are calculated as

$$J_*(|\Phi^\pm\rangle) = \frac{\gamma^2}{[(2+\sqrt{2})\gamma + \mathcal{U}]^2}, \ J_*(|\Psi^+\rangle) = \frac{4\gamma^2}{(4\sqrt{2}\gamma + \mathcal{U})^2},$$

and $J_*(|\Psi^-\rangle) = 0$. Here we assumed that, for each case of the Bell state, an appropriate control Hamiltonian H is chosen so that the same magnitude of control, $\mathcal{U}$, appears in the expression of J_* for fair comparison. Hence, the Bell states, which ideally have the same amount of entanglement, have different reachability properties under realistic decoherence. Clearly, in our case $|\Psi^-\rangle$ is the best target state; this is identical to the dark state of L and is indeed reachable. Also $J_*(|\Phi^\pm\rangle) < J_*(|\Psi^+\rangle)$ holds for all γ and $\mathcal{U}$, showing that $|\Psi^+\rangle$ is the most fragile Bell state under the collective decay process. On the other hand, if each qubit experiences a local decay, which is modeled as $L_1 = \sqrt{\gamma}\sigma_- \otimes I$ and $L_2 = \sqrt{\gamma} I \otimes \sigma_-$ rather than the global decay $L = \sqrt{\gamma}(\sigma_- \otimes +I \otimes \sigma_-)$, then we have $J_* = \gamma^2/\{(2+\sqrt{2})\gamma + \mathcal{U}\}^2$ for all Bell states. That is, in this case there is no difference between the Bell states, in view of the reachability property.

It is also interesting to see the case of MBF [13, 45]. In particular we limit the system to a pair of symmetric qubits, which is identical to a qutrit composed of three distinguishable states $|E\rangle = [1, 0, 0]^\top$, $|S\rangle = [0, 1, 0]^\top$, and $|G\rangle = [0, 0, 1]^\top$. Note that $|S\rangle$ corresponds to the entangled state between two qubits. Here we limit the target state to the following real vector:

$$|\psi\rangle = [\sin(\theta/2)\cos(\varphi/2), \ \cos(\theta/2), \ \sin(\theta/2)\sin(\varphi/2)]^\top,$$

where $0 \le \theta, \varphi \le \pi$. The MBF setup considered here is given by

$$H = J_y, \ M = \sqrt{\kappa} J_z, \ L = \sqrt{\gamma} J_-,$$

where $J_y = i(|S\rangle\langle E| + |G\rangle\langle S|)/\sqrt{2} + \text{h.c.}$, $J_z = |E\rangle\langle E| - |G\rangle\langle G|$, and $J_- = \sqrt{2}(|S\rangle\langle E| + |G\rangle\langle S|)$. The continuous measurement through the system-probe coupling represented by M, ideally, induces the probabilistic state reduction to $|E\rangle$, $|S\rangle$, or $|G\rangle$. The decoherence process L represents the ladder-type decay $|E\rangle \to |S\rangle \to |G\rangle$. In this setting the lower bound $J_*(|\psi\rangle)$ can be explicitly calculated as a function of (θ, φ) and is illustrated in Fig. 2. As in the qubit case, $J_*(|\psi\rangle)$ takes the maximum at $|E\rangle$ when $\kappa = 0$ (Fig. 2(a)), but $J_*(|E\rangle)$ can be drastically decreased by taking a non-zero κ (Fig. 2(b)); that is, the measurement enables us to combat with the decoherence and have chance to closely approach to $|E\rangle$ via a MBF. However, this strategy does not work for the case of $|S\rangle$, because $J_*(|\psi\rangle)$ is independent to κ at $\theta = 0$. In general, if the target $|\psi\rangle$ is an eigenstate of $M = M^\dagger$ with small eigenvalue, then the term related to M takes a small value as well in $\mathcal{A}$ and zero in $\mathcal{E}$. In particular for the dark state satisfying $M|\psi\rangle = 0$, $J_*(|\psi\rangle)$ is independent on M, hence in this case the measurement does not at all help to decrease J_*. Conversely, for an eigenstate of M with large eigenvalue, i.e., a bright state $|E\rangle$ in our case, the term related to M in $\mathcal{A}$ takes a large number and eventually J_* becomes small, implying that we could closely approach to such a state via some MBF control even under decoherence.

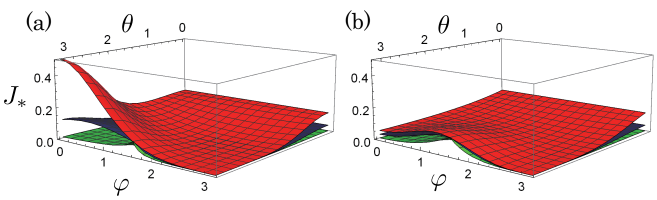

FIG. 2: The lower bound $J_*(|\psi\rangle)$ as a function of (θ, φ) for (a) $\kappa = 0$ and (b) $\kappa = 1$, in the unit $\gamma = 1$. In both cases the curved surface corresponds to $\bar{u} = 0, 1, 5$ from top to bottom.

C. Atomic ensemble

Next we study an ensemble composed of N identical atoms. The basic operators for describing this system are the angular momentum operator J_i $(i = x, y, z)$ satisfying e.g., $[J_x, J_y] = iJ_z$, the magnitude $\mathbf{J}^2 = J_x^2 + J_y^2 + J_z^2$, and the ladder operator $J_- = J_x - iJ_y$. Here we focus on the Dicke states $|l, m\rangle$, which are the common eigenstates of J_z and $\mathbf{J}^2$ defined by $J_z|l, m\rangle = m|l, m\rangle$ and $\mathbf{J}^2|l, m\rangle = l(l+1)|l, m\rangle$ where $|m| \le l \le N/2$ [46]. Recall, for N even, that $|N/2, N/2\rangle$ corresponds to the coherent spin state (CSS) $|\uparrow\rangle^{\otimes N}$, i.e., the separable state with all the spins pointing along the z axis, while $|N/2, 0\rangle$ is highly entangled.

It was proven in [9, 15] that, for the ideal system subjected to the SME (2) with $(H, M, L) = (J_y, \sqrt{\kappa}J_z, 0)$, the Dicke state $|N/2, m\rangle$ for arbitrary $m \in [-N/2, N/2]$ can be deterministically generated by an appropriate MBF control. Now using the lower bound J_* we can evaluate how much this MBF control method could work under decoherence. Let $L = \sqrt{\gamma}J_-$. Then, the lower bound for $|\psi\rangle = |l, m\rangle$ is calculated as

$$J_* = \frac{1}{2}\left[\frac{\gamma(l^2 + l - m^2 + m)}{2\kappa m^2 + 2\gamma(l^2 + l - m^2) + \bar{u}\sqrt{l^2 + l - m^2}}\right]^2.$$

Figure 3(a) shows the case of $N = 20$ atoms, for the target Dicke state $|\psi\rangle = |10, m\rangle$. We observe that, as in the previous studies, the measurement drastically decreases J_* especially for the state with large $|m|$, e.g., the CSS $|10, 10\rangle$. Meanwhile the lower bound at around the entangled state $|10, 0\rangle$ is not almost affected by the measurement. Actually in general, for a Dicke state with large $|m| \lesssim l = N/2$, such as the CSS, the measurement term proportional to κ is dominant in the denominator of J_*, while for highly entangled Dicke states with $m \sim 0$ the decoherence term proportional to γ becomes dominant. In particular,

$$J_*(|N/2, N/2\rangle) = \left[\frac{\sqrt{2}\gamma N}{\kappa N^2 + 2\gamma N + \bar{u}\sqrt{2N}}\right]^2,$$

$$J_*(|N/2, 0\rangle) = \frac{1}{2}\left[\frac{\gamma(N^2 + 2N)}{2\gamma N^2 + 4\gamma N + 2\bar{u}\sqrt{N^2 + 2N}}\right]^2.$$

Therefore, for a large ensemble limit $N \to \infty$, we have $J_*(|N/2, N/2\rangle) \to 0$ and $J_*(|N/2, 0\rangle) \to 1/8$. Note that this fundamental bound $J_* = 1/8$ is applied to all highly entangled Dicke states satisfying $m \sim 0$ and $l \lesssim N/2 \gg 1$. That is, while no limitation appears for the case of CSS thanks to the measurement effect, generating those highly entangled Dicke states is strictly prohibited, irrespective of the use of measurement and control. This result implies that, in practice, there exists a strict limitation in quantum magnetometry that utilizes a highly entangled Dicke state [47].

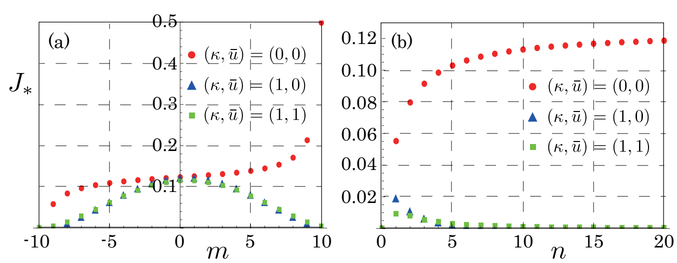

FIG. 3: The lower bound J_* for (a) the atomic Dicke states and (b) the optical Fock states, in the unit $\gamma = 1$.

Another important subject in quantum metrology is the frequency standard, where the GHZ state $|\text{GHZ}\rangle = (|\uparrow\rangle^{\otimes N} + |\downarrow\rangle^{\otimes N})/\sqrt{2}$ is used for estimating the atomic frequency, over the standard quantum limit attained with the use of the product state $|+\rangle^{\otimes N} = (|\uparrow\rangle/\sqrt{2} + |\downarrow\rangle/\sqrt{2})^{\otimes N}$ [48]. The main issue of this technique is that the estimation performance is severely limited [49, 50] due to the dephasing noise, which affects on both the state preparation process and the free-precession process. Here we characterize the performance degradation occurred in the former process, using the lower bound J_*. In the usual setup where no continuous monitoring is applied, the realistic system obeys the master equation $d\bar{\rho}/dt = -i[H,\bar{\rho}]+\mathcal{D}[L]\bar{\rho}$, where $L=\sqrt{\gamma}J_z$ represents the dephasing process and H is a system Hamiltonian representing an open-loop control. Then the lower bounds for the above two states are given by

$$J_*(|+\rangle^{\otimes N}) = \left(\frac{\gamma N}{\sqrt{2}\gamma N + \gamma\sqrt{6N^2-4N} + 4\mathcal{U}}\right)^2,$$
$$J_*(|\mathrm{GHZ}\rangle) = \left(\frac{\gamma N^2}{2\sqrt{2}\gamma N^2 + 4\mathcal{U}}\right)^2.$$

Thus, irrespective of control, $J_*(|+\rangle^{\otimes N}) \to 1/(8+4\sqrt{3})$ and $J_*(|\mathrm{GHZ}\rangle) \to 1/8$ in the limit $N\to\infty$, under the assumption that $\mathcal{U}$ is of the order at most $\sqrt{N}$ and N, respectively. Hence, the GHZ state is harder to prepare than the product one, and this gap would erase the quantum advantage obtained using the GHZ state in the ideal setting. In both cases, the estimation performance must be severely limited in the presence of decoherence, if the total time taken for state preparation and free-precession dynamics becomes long; thus, these two processes have to be carried out in as short time as possible.

D. Fock state

The last case study is the problem for generating a Fock state in an optical cavity. In the setup of [11, 12, 14], the conditional cavity state obeys the SME (2) with $M=\sqrt{\kappa}a^\dagger a$ and $H=i(a^\dagger - a)$, where a is the annihilation operator; then it was proven in the ideal case (i.e., $L=0$) that, by choosing an appropriate MBF input u_t, one can deterministically steer the state to a target Fock state $|n\rangle$. Now the lower bound J_* can be used to evaluate the performance of this MBF control in the presence of decoherence. A typical decoherence is the photon leakage modeled by $L=\sqrt{\gamma}a$. In this setting, J_* for $|\psi\rangle=|n\rangle$ is calculated as

$$J_*(|n\rangle) = \frac{1}{2}\left[\frac{\gamma n}{2\kappa n^2 + \gamma(2n+1) + \bar{u}\sqrt{4n+2}}\right]^2.$$

Figure 3(b) plots J_* in the case $\gamma=1$. As in the previous studies, the measurement drastically decreases J_*. However, $J_*\sim 0$ for large Fock states $|n\rangle$ ($n\gtrsim 5$) does not necessarily mean that those states can be exactly stabilized via MBF; rather a large Fock state might be hard to prepare compared to a small one such as $|1\rangle$. Hence, in this problem the lower bound only for small Fock states $|n\rangle$ ($n\lesssim 4$) has a practical meaning.

IV. CONCLUSION

In this paper, we have derived the general lower bound J_* of the distance between the controlled quantum state under decoherence and an arbitrary target state. The lower bound can be straightforwardly calculated and used as a useful guide for engineering open quantum systems; for instance, in the reservoir engineering scenario, the system should be configured so that J_* takes the minimum for a given target state. An important remaining work is to explore an achievable lower bound and develop an efficient method for synthesizing the controller (e.g., the MBF control input) that achieves the bound.

This work was supported in part by JST PRESTO No. JPMJPR166A.

Appendix A: Proof of the theorem

We prove the theorem in the MBF setting; the open-loop control and reservoir engineering case is obtained by simply setting the control signal u_t to be independent to the conditional state ρ_t.

First, the infinitesimal change of the random variable

$$j_t = 1-\mathrm{Tr}(Q\rho_t), \quad Q=|\psi\rangle\langle\psi|,$$

where ρ_t is the solution of the stochastic master equation (2) and $|\psi\rangle$ is the target, is given by

$$\begin{aligned} dj_t &= -\mathrm{Tr}(Qd\rho_t) \\ &= -\mathrm{Tr}\big\{Q\big(-i[u_tH,\rho_t]dt + \mathcal{D}[L]\rho_t dt \\ &\qquad + \mathcal{D}[M]\rho_t dt + \mathcal{H}[M]\rho_t dW_t\big)\big\} \\ &= \mathrm{Tr}\big(iu_t[Q,H]\rho_t\big)dt - \mathrm{Tr}\big(Q\mathcal{D}[L]\rho_t\big)dt \\ &\qquad - \mathrm{Tr}\big(Q\mathcal{D}[M]\rho_t\big)dt - \mathrm{Tr}\big(Q\mathcal{H}[M]\rho_t\big)dW_t. \end{aligned} \quad \text{(A1)}$$

The classical stochastic process (the Wiener process) W_t satisfies the Ito rule $dW_t^2=dt$ and $\mathbb{E}(W_t)=0$. The ensemble average of this equation, with respect to W_t, is thus

$$\begin{aligned} \frac{d\mathbb{E}(j_t)}{dt} &= \mathrm{Tr}\big\{i[Q,H]\mathbb{E}(u_t\rho_t)\big\} - \mathrm{Tr}\big\{Q\mathcal{D}[L]\mathbb{E}(\rho_t)\big\} \\ &\qquad - \mathrm{Tr}\big\{Q\mathcal{D}[M]\mathbb{E}(\rho_t)\big\}. \end{aligned} \quad \text{(A2)}$$

Note again that u_t is a function of ρ_t in the context of MBF control.

In the proof we often use the Schwarz inequality for matrices (or bounded operators) X and Y;

$$\|X\|_{\mathrm{F}}\cdot\|Y\|_{\mathrm{F}} \geq \frac{1}{2}\Big|\mathrm{Tr}(X^\dagger Y + Y^\dagger X)\Big|,$$

where $\|X\|_{\mathrm{F}} := \sqrt{\mathrm{Tr}(X^\dagger X)}$ is the Frobenius norm. In particular, if X and Y are Hermitian, then $\|X\|_{\mathrm{F}}\cdot\|Y\|_{\mathrm{F}} \geq |\mathrm{Tr}(XY)|$ holds. The following inequality is also often used:

$$\begin{aligned} \|\rho_t - Q\|_{\mathrm{F}} &= \sqrt{\mathrm{Tr}[(\rho_t-Q)^2]} = \sqrt{\mathrm{Tr}(\rho_t^2 - 2\rho_t Q + Q^2)} \\ &\leq \sqrt{2-2\mathrm{Tr}(\rho_t Q)} = \sqrt{2j_t}, \end{aligned}$$

where $\mathrm{Tr}(\rho_t^2) \leq 1$ and $\mathrm{Tr}(Q^2) = \mathrm{Tr}(Q) = 1$ are used.

We begin with calculating a lower bound of the first term in the most right-hand side of Eq. (A1) as follows:

$$\begin{aligned}
\mathrm{Tr}\big(iu_t[Q,H]\rho_t\big) &\geq -\bar{u}\Big|\mathrm{Tr}\big(i[Q,H]\rho_t\big)\Big| \\
&= -\bar{u}\Big|\mathrm{Tr}\big\{i[Q,H](\rho_t - Q)\big\}\Big| \\
&\geq -\bar{u}\|i[H,Q]\|_{\mathrm{F}} \cdot \|\rho_t - Q\|_{\mathrm{F}} \\
&= -\bar{u}\sqrt{\mathrm{Tr}\{(iHQ - iQH)^2\}} \cdot \sqrt{2j_t} \\
&\geq -2\bar{u}\sqrt{\langle\psi|H^2|\psi\rangle - \langle\psi|H|\psi\rangle^2} \cdot \sqrt{j_t},
\end{aligned}$$

where $\bar{u} := \max\{|u_t|\}$ is the upper bound of the control input. Then, by taking the ensemble average of this equation with respect to W_t, we have

$$\begin{aligned}
&\mathrm{Tr}\big\{i[Q,H]\mathbb{E}(u_t\rho_t)\big\} \\
&\qquad \geq -2\bar{u}\sqrt{\langle\psi|H^2|\psi\rangle - \langle\psi|H|\psi\rangle^2} \cdot \mathbb{E}(\sqrt{j_t}) \\
&\qquad \geq -2\bar{u}\sqrt{\langle\psi|H^2|\psi\rangle - \langle\psi|H|\psi\rangle^2} \cdot \sqrt{\mathbb{E}(j_t)},
\end{aligned}$$

where $\mathbb{E}(\sqrt{j_t}) \leq \sqrt{\mathbb{E}(j_t)}$ is used. Next, the second term in the most right-hand side of Eq. (A1) can be lower bounded as follows;

$$\begin{aligned}
&-\mathrm{Tr}\big(Q\mathcal{D}[L]\rho_t\big) = -\mathrm{Tr}\Big[Q\big(L\rho_t L^\dagger - \frac{1}{2}\rho_t L^\dagger L - \frac{1}{2}L^\dagger L\rho_t\big)\Big] \\
&= -\mathrm{Tr}\big[L^\dagger QL(\rho_t - Q)\big] - \mathrm{Tr}(L^\dagger QLQ) + \mathrm{Tr}(QL^\dagger LQ) \\
&\quad - \frac{1}{2}\mathrm{Tr}\big[(Q-\rho_t)L^\dagger LQ + (L^\dagger LQ)^\dagger(Q-\rho_t)\big] \\
&\geq -\|L^\dagger QL\|_{\mathrm{F}} \cdot \|\rho_t - Q\|_{\mathrm{F}} - \|L^\dagger LQ\|_{\mathrm{F}} \cdot \|\rho_t - Q\|_{\mathrm{F}} \\
&\quad + \mathrm{Tr}(L^\dagger LQ) - \mathrm{Tr}(L^\dagger QLQ) \\
&\geq -\Big\{\sqrt{\mathrm{Tr}\big[(L^\dagger QL)^2\big]} + \sqrt{\mathrm{Tr}\big[(L^\dagger LQ)^\dagger(L^\dagger LQ)\big]}\Big\}\sqrt{2j_t} \\
&\quad + \mathrm{Tr}(L^\dagger LQ) - \mathrm{Tr}(L^\dagger QLQ) \\
&= -\sqrt{2}\left(\langle\psi|LL^\dagger|\psi\rangle + \sqrt{\langle\psi|(L^\dagger L)^2|\psi\rangle}\right)\sqrt{j_t} \\
&\quad + \langle\psi|L^\dagger L|\psi\rangle - |\langle\psi|L|\psi\rangle|^2 \\
&= -\sqrt{2}\left(\|L^\dagger|\psi\rangle\|^2 + \|L^\dagger L|\psi\rangle\|\right)\sqrt{j_t} \\
&\quad + \|L|\psi\rangle\|^2 - |\langle\psi|L|\psi\rangle|^2.
\end{aligned}$$

Hence again it follows from $\mathbb{E}(\sqrt{j_t}) \leq \sqrt{\mathbb{E}(j_t)}$ that

$$\begin{aligned}
&-\mathrm{Tr}\big\{Q\mathcal{D}[L]\mathbb{E}(\rho_t)\big\} \\
&\qquad \geq -\sqrt{2}\left(\|L^\dagger|\psi\rangle\|^2 + \|L^\dagger L|\psi\rangle\|\right)\sqrt{\mathbb{E}(j_t)} \\
&\qquad\quad + \|L|\psi\rangle\|^2 - |\langle\psi|L|\psi\rangle|^2.
\end{aligned}$$

The same inequality as above, with L replaced by M, holds. Hence, combining the above three inequalities with Eq. (A2) and using the definition $J_t = \mathbb{E}(j_t) = 1 - \mathrm{Tr}\big\{Q\mathbb{E}(\rho_t)\big\} = 1 - \mathrm{Tr}(Q\bar{\rho}_t)$, we end up with

$$\frac{dJ_t}{dt} \geq -\mathcal{U}\sqrt{J_t} - \mathcal{A}\sqrt{J_t} + \mathcal{E}, \tag{A3}$$

where

$$\begin{aligned}
\frac{\mathcal{A}}{\sqrt{2}} &= \|L^\dagger|\psi\rangle\|^2 + \|L^\dagger L|\psi\rangle\| + \|M^\dagger|\psi\rangle\|^2 + \|M^\dagger M|\psi\rangle\|, \\
\mathcal{U} &= 2\bar{u}\sqrt{\langle\psi|H^2|\psi\rangle - \langle\psi|H|\psi\rangle^2}, \quad \bar{u} := \max\{|u_t|\}, \\
\mathcal{E} &= \|L|\psi\rangle\|^2 - |\langle\psi|L|\psi\rangle|^2 + \|M|\psi\rangle\|^2 - |\langle\psi|M|\psi\rangle|^2.
\end{aligned}$$

To obtain the lower bound of J_t in the limit $t \to \infty$, let us consider the function $f(x) = -\mathcal{U}\sqrt{x} - \mathcal{A}\sqrt{x} + \mathcal{E}$ in the range $x \in [0,1]$. Clearly, $f(x)$ is a monotonically decreasing function with respect to x. Also, from the Schwarz inequality $\|L|\psi\rangle\|^2 - |\langle\psi|L|\psi\rangle|^2 \geq 0$, we have $f(0) = \mathcal{E} \geq 0$. Moreover, $f(1) = \mathcal{E} - \mathcal{A} - \mathcal{U} \leq 0$ holds, because

$$\begin{aligned}
\|L|\psi\rangle\|^2 &= \mathrm{Tr}(L^\dagger LQ) \\
&= \frac{1}{2}\Big\{\mathrm{Tr}\big[(L^\dagger LQ)^\dagger Q\big] + \mathrm{Tr}\big[Q^\dagger(L^\dagger LQ)\big]\Big\} \\
&\leq \|L^\dagger LQ\|_{\mathrm{F}} \cdot \|Q\|_{\mathrm{F}} = \|L^\dagger LQ\|_{\mathrm{F}} = \|L^\dagger L|\psi\rangle\|,
\end{aligned}$$

which clearly leads to $\mathcal{E} - \mathcal{A} \leq 0$ and accordingly $\mathcal{E} - \mathcal{A} - \mathcal{U} \leq 0$. In what follows we consider the case $\mathcal{E} > 0$. Then, from the above properties of $f(x)$, the equation $f(J_*) = 0$ has a unique solution J_* in $(0,1]$. Now suppose that $J_\tau < J_*$ at a given time τ; then Eq. (A3) leads to

$$\begin{aligned}
\frac{dJ_t}{dt}\Big|_{t=\tau} &\geq -\mathcal{U}\sqrt{J_\tau} - \mathcal{A}\sqrt{J_\tau} + \mathcal{E} \\
&> -\mathcal{U}\sqrt{J_*} - \mathcal{A}\sqrt{J_*} + \mathcal{E} = 0.
\end{aligned}$$

This means that J_t locally increases in time for $t \geq \tau$. Because this argument is true for any τ such that the inequality $J_\tau < J_*$ holds, J_t increases until J_t coincides with J_*; i.e., $\lim_{t\to\infty} J_t = J_*$. On the other hand for the range such that $J_\tau \geq J_*$ the inequality (A3) does not say anything about the local time evolution of J_t for $t \geq \tau$. As a result, in the long time limit we have

$$\lim_{t\to\infty} J_t \geq J_* = \left(\frac{\mathcal{E}}{\mathcal{A}+\mathcal{U}}\right)^2.$$

Note that this inequality is valid for the case $\mathcal{E} = 0$ as well.

Next we prove that $J_t \geq J_*$ holds for all $t \in [t_0, \infty)$, if the initial value J_{t_0} is bigger than J_*. For the proof we use the following fact:

Comparison Theorem [51]: Consider the following real-valued 1-dimensional ordinary differential equation:

$$\frac{dx(t)}{dt} = f(x(t)), \quad t \in [t_0, \infty).$$

If $dx_1(t)/dt \leq f(x_1(t))$ and $f(x_2(t)) \leq dx_2(t)/dt$, $\forall t \in [t_0, \infty)$ hold for the initial values satisfying $x_1(t_0) \leq x_2(t_0)$, then $x_1(t) \leq x_2(t)$ holds for $\forall t \in [t_0, \infty)$.

Proof: A contradiction argument will be used. Suppose that there exists $t \in [t_0, \infty)$ such that $x_1(t) > x_2(t)$.

Then, because $x_1(t_0) \le x_2(t_0)$, there exists $T \ge t_0$ satisfying $x_1(T) = x_2(T)$. Moreover, there exists $h > 0$ such that $x_1(T+h) > x_2(T+h)$ holds. Hence,

$$\begin{aligned}\frac{dx_1(t)}{dt}\Big|_{T+0} &= \lim_{h\to+0}\frac{x_1(T+h)-x_1(T)}{h}\\ &> \lim_{h\to+0}\frac{x_2(T+h)-x_2(T)}{h} = \frac{dx_2(t)}{dt}\Big|_{T+0}.\end{aligned}$$

Then, from the assumption of the theorem,

$$f\left(x_1(T)\right) \ge \frac{dx_1(t)}{dt}\Big|_{T+0} > \frac{dx_2(t)}{dt}\Big|_{T+0} \ge f\left(x_2(T)\right).$$

This is a contradiction to $x_1(T) = x_2(T)$. Therefore $x_1(t) \le x_2(t)$ holds for $\forall t \in [t_0, \infty)$. ■

Let us apply the above comparison theorem to the case $f(x) = -\mathcal{U}\sqrt{x} - \mathcal{A}\sqrt{x} + \mathcal{E}$. Assuming that $x_1(t_0) = J_* = \{\mathcal{E}/(\mathcal{A}+\mathcal{U})\}^2$, we have $dx_1(t)/dt = f(x_1(t)) = 0$ and $x_1(t) = x_1(t_0) = J_*$ for $\forall t \in [t_0, \infty)$. Also we take $x_2(t) = J_t$, which satisfies the inequality (A3), i.e., $dx_2(t)/dt \ge f(x_2(t))$. Thus, from the comparison theorem, if $J_* = x_1(t_0) \le x_2(t_0) = J_{t_0}$, then $J_* = x_1(t) \le x_2(t) = J_t$ for all $t \in [t_0, \infty)$. That is, we obtain

$$J_t \ge J_* = \left(\frac{\mathcal{E}}{\mathcal{A}+\mathcal{U}}\right)^2, \quad \forall t \in [t_0, \infty).$$

This is end of the proof of the theorem.

Appendix B: Generalization of the theorem

If the system dynamics is validly modeled by the stochastic master equation

$$\begin{aligned}d\rho_t = &- i\Big[\sum_j u_{j,t}H_j, \rho_t\Big]dt + \sum_j \mathcal{D}[L_j]\rho_t dt\\ &+ \sum_j \mathcal{D}[M_j]\rho_t dt + \sum_j \mathcal{H}[M_j]\rho_t dW_t,\end{aligned}$$

for the MBF case or the master equation

$$\frac{d\bar\rho_t}{dt} = -i\Big[\sum_j u_{j,t}H_j, \bar\rho_t\Big] + \sum_j \mathcal{D}[L_j]\bar\rho_t + \sum_j \mathcal{D}[M_j]\bar\rho_t,$$

for the open-loop control or reservoir engineering case, by the straightforward extension of the above discussion we find that the lower bound is given by $J_* = \mathcal{E}^2/(\mathcal{A}+\mathcal{U})^2$ with

$$\begin{aligned}\mathcal{A} &= \sqrt{2}\sum_j \left(\|L_j^\dagger|\psi\rangle\|^2 + \|L_j^\dagger L_j|\psi\rangle\|\right)\\ &\quad +\sqrt{2}\sum_j \left(\|M_j^\dagger|\psi\rangle\|^2 + \|M_j^\dagger M_j|\psi\rangle\|\right),\\ \mathcal{U} &= 2\sum_j \bar u_j\sqrt{\langle\psi|H_j^2|\psi\rangle - \langle\psi|H_j|\psi\rangle^2},\\ &\quad \bar u_j = \max\{|u_{j,t}|\},\\ \mathcal{E} &= \sum_j \left(\|L_j|\psi\rangle\|^2 - |\langle\psi|L_j|\psi\rangle|^2\right)\\ &\quad +\sum_j \left(\|M_j|\psi\rangle\|^2 - |\langle\psi|M_j|\psi\rangle|^2\right).\end{aligned}$$

Using this result we can involve a fixed system Hamiltonian in addition to controllable Hamiltonians; in the simple case where the Hamiltonian is given by $H_0 + u_t H_1$ with H_0 a fixed system Hamiltonian, we have

$$\begin{aligned}\mathcal{U} &= 2\sqrt{\langle\psi|H_0^2|\psi\rangle - \langle\psi|H_0|\psi\rangle^2}\\ &\quad + 2\bar u\sqrt{\langle\psi|H_1^2|\psi\rangle - \langle\psi|H_1|\psi\rangle^2},\end{aligned}$$

with $\bar u = \max\{|u_t|\}$.

Appendix C: A measurement-based feedback control law

Let us consider the continuously-monitored system whose dynamics is given by the following SME:

$$d\rho_t = -i[u_t J_y, \rho_t]dt + \mathcal{D}[J_z]\rho_t dt + \mathcal{H}[J_z]\rho_t dW_t,$$

where J_y and J_z are the angular momentum operators. Now the target state $|\psi\rangle$ is set to be one of the eigenstates of J_z. In Ref. [15] the authors proposed the following feedback control law that deterministically steers the conditional state ρ_t to the target state:

1. $u_t = -\alpha \mathrm{Tr}\{i[J_y, \rho_t]Q\}$ if $\mathrm{Tr}(Q\rho_t) \ge \beta$,
2. $u_t = \alpha$ if $\mathrm{Tr}(Q\rho_t) \le \beta/2$,
3. If $\rho_t \in \mathcal{B} = \{\rho \mid \beta/2 < \mathrm{Tr}(Q\rho_t) < \beta\}$, then $u_t = -\alpha\mathrm{Tr}\{i[J_y, \rho_t]Q\}$ in the case ρ_t last entered $\mathcal{B}$ through the boundary $\mathrm{Tr}(Q\rho) = \beta$, and $u_t = \alpha$ otherwise,

where α and β are positive constants. In fact, it was proven that there exists $\beta > 0$ such that $\rho_t \to Q = |\psi\rangle\langle\psi|$ almost surely.

Here we calculate the upper bound $\bar u$ of the above MBF control input, in the qubit control problem discussed in

Sec. III A. First we have

$$\begin{aligned}\mathrm{Tr}(\Delta\sigma_y^2\rho_t) &= \mathrm{Tr}(\sigma_y^2\rho_t) - [\mathrm{Tr}(\sigma_y\rho_t)]^2 \\ &= 1 - [\mathrm{Tr}(\sigma_y\rho_t)]^2 \le 1, \\ \mathrm{Tr}(\Delta Q^2\rho_t) &= \mathrm{Tr}(Q^2\rho_t) - [\mathrm{Tr}(Q\rho_t)]^2 \\ &= \mathrm{Tr}(Q\rho_t) - [\mathrm{Tr}(Q\rho_t)]^2 \\ &= (1-J_t)J_t \le \frac{1}{4}.\end{aligned}$$

Then, the Robertson inequality $\mathrm{Tr}(\Delta\sigma_y^2\rho_t)\mathrm{Tr}(\Delta Q^2\rho_t) \ge |\mathrm{Tr}\{i[\sigma_y, Q]\rho_t\}|^2/4$ leads to

$$\begin{aligned}\Big| -\alpha\mathrm{Tr}\left\{i[J_y,\rho_t]Q\right\}\Big| &\le 2\alpha\sqrt{\mathrm{Tr}(\Delta\sigma_y^2\rho_t)}\sqrt{\mathrm{Tr}(\Delta Q^2\rho_t)} \\ &\le 2\alpha\cdot\frac{1}{2} = \alpha.\end{aligned}$$

Hence, together with the other case of input, we have $\bar{u} = \max\{|u_t|\} = \alpha$; in the numerical simulation depicted in Fig. 1(c) in the main text, $\bar{u} = \alpha = 1$ was chosen.

Appendix D: Detailed calculations of the lower bound

1. Qubit

The target state is $|\psi\rangle = [\cos\theta,\ e^{i\varphi}\sin\theta]^\top$ $(0 \le \theta < \pi/2, 0 \le \varphi < 2\pi)$, and the system operators are $H = \sigma_y$, $M = \sqrt{\kappa}\sigma_z$, and $L = \sqrt{\gamma}\sigma_-$. Then we have

$$\begin{aligned}\frac{\mathcal{A}}{\sqrt{2}} &= \|L^\dagger|\psi\rangle\|^2 + \|L^\dagger L|\psi\rangle\| + \|M^\dagger|\psi\rangle\|^2 + \|M^\dagger M|\psi\rangle\| \\ &= 2\kappa + \gamma\sin^2\theta + \gamma\cos\theta, \\ \mathcal{U} &= 2\bar{u}\sqrt{\langle\psi|H^2|\psi\rangle - \langle\psi|H|\psi\rangle^2} \\ &= 2\bar{u}\sqrt{1-\sin^2 2\theta\sin^2\varphi}, \\ \mathcal{E} &= \|L|\psi\rangle\|^2 - |\langle\psi|L|\psi\rangle|^2 + \|M|\psi\rangle\|^2 - |\langle\psi|M|\psi\rangle|^2 \\ &= \kappa\sin^2 2\theta + \gamma\cos^4\theta.\end{aligned}$$

2. Qutrit

The target state is limited to the real vector $|\psi\rangle = [\sin(\theta/2)\cos(\varphi/2), \cos(\theta/2), \sin(\theta/2)\sin(\varphi/2)]^\top$. The system operators are given by

$$H = \frac{1}{\sqrt{2}}\begin{bmatrix} 0 & -i & 0 \\ i & 0 & -i \\ 0 & i & 0\end{bmatrix},\ M = \sqrt{\kappa}\begin{bmatrix} 1 & 0 & 0 \\ 0 & 0 & 0 \\ 0 & 0 & -1\end{bmatrix},$$
$$L = \sqrt{\gamma}\begin{bmatrix} 0 & 0 & 0 \\ 1 & 0 & 0 \\ 0 & 1 & 0\end{bmatrix}.$$

Then, from the definition of $\mathcal{A}$, $\mathcal{U}$, and $\mathcal{E}$, we have

$$\begin{aligned}\frac{\mathcal{A}}{\sqrt{2}} &= \kappa\left(\sin^2\frac{\theta}{2} + \sin\frac{\theta}{2}\right) \\ &\quad + \gamma\left(\cos^2\frac{\theta}{2} + \sin^2\frac{\theta}{2}\sin^2\frac{\varphi}{2} + \sqrt{\sin^2\frac{\theta}{2}\cos^2\frac{\varphi}{2} + \cos^2\frac{\theta}{2}}\right), \\ \mathcal{U} &= \sqrt{2}\bar{u}\sqrt{1+\cos^2\frac{\theta}{2} - \sin^2\frac{\theta}{2}\sin\varphi}, \\ \mathcal{E} &= \kappa\left(\sin^2\frac{\theta}{2} + \sin\frac{\theta}{2}\right) \\ &\quad + \gamma\left(\sin^2\frac{\theta}{2}\sin^2\frac{\varphi}{2} + \cos^2\frac{\theta}{2} + \sqrt{\sin^2\frac{\theta}{2}\cos^2\frac{\varphi}{2} + \cos\frac{\theta}{2}}\right).\end{aligned}$$

3. Dicke state

The target is the Dicke state $|l,m\rangle$, and the system operators are $H = J_y$, $M = \sqrt{\kappa}J_z$, and $L = \sqrt{\gamma}J_-$. Recall that $|l,m\rangle$ is a common eigenvector of J_z and the orbital angular momentum operator $\mathbf{J}^2 = J_x^2 + J_y^2 + J_z^2$;

$$J_z|l,m\rangle = m|l,m\rangle,\quad \mathbf{J}^2|l,m\rangle = l(l+1)|l,m\rangle.$$

Also the raising and lowering operators $J_\pm = J_x \pm iJ_y$ act on $|l,m\rangle$ as follows:

$$J_\pm|l,m\rangle = \sqrt{(l\mp m)(l\pm m+1)}|l,m\pm 1\rangle.$$

The following equations are also used;

$$\begin{aligned}J_+J_- &= (J_x+iJ_y)(J_x-iJ_y) \\ &= J_x^2 + J_y^2 - iJ_xJ_y + iJ_yJ_x \\ &= \mathbf{J}^2 - J_z^2 - i[J_x,J_y] = \mathbf{J}^2 - J_z^2 + J_z,\end{aligned}$$

and likewise $J_-J_+ = \mathbf{J}^2 - J_z^2 - J_z$. Then we have

$$\begin{aligned}\mathcal{A} &= \sqrt{2}\Big(\kappa\|J_z|l,m\rangle\|^2 + \kappa\|J_z^2|l,m\rangle\| \\ &\qquad + \gamma\|J_-^\dagger|l,m\rangle\|^2 + \gamma\|J_-^\dagger J_-|l,m\rangle\|\Big) \\ &= \sqrt{2}\Big[\kappa m^2 + \kappa m^2 + \gamma\{l(l+1) - m^2 - m\} \\ &\qquad + \gamma\{l(l+1) - m^2 + m\}\Big] \\ &= \sqrt{2}\left\{2\kappa m^2 + 2\gamma(l^2+l-m^2)\right\}, \\ \mathcal{U} &= \bar{u}\sqrt{\Big\|(J_-^\dagger - J_-)|l,m\rangle\Big\|^2 - \Big|\langle l,m|(J_-^\dagger - J_-)|l,m\rangle\Big|^2} \\ &= \bar{u}\sqrt{\{(l-m)(l+m+1) + (l+m)(l-m+1)\}} \\ &= \sqrt{2}\bar{u}\sqrt{l^2+l-m^2}, \\ \mathcal{E} &= \kappa\|J_z|l,m\rangle\|^2 - \kappa\left|\langle l,m|J_z|l,m\rangle\right|^2 \\ &\qquad + \gamma\|J_-|l,m\rangle\|^2 - \gamma\left|\langle l,m|J_-|l,m\rangle\right|^2 \\ &= \kappa m^2 - \kappa m^2 + \gamma(l+m)(l-m+1) \\ &= \gamma(l^2+l-m^2+m).\end{aligned}$$

4. Product state of the spin superposition

The target is the product state of the spin superposition, $|+\rangle^{\otimes N}$, where $|+\rangle = (|\uparrow\rangle + |\downarrow\rangle)/\sqrt{2}$. The system is driven by the dephasing process $L = \sqrt{\gamma} J_z$ and an appropriate control Hamiltonian H, but it is not subjected to continuous monitoring and subsequent MBF (i.e., $M = 0$). Recall that J_z can be represented as

$$J_z = \frac{1}{2}\sum_{j=1}^{N} \sigma_z^{(j)} = \frac{1}{2}\sum_{j=1}^{N} (I \otimes \ldots \otimes \sigma_z \otimes \ldots \otimes I), \quad \text{(D1)}$$

where the Pauli matrix σ_z appears in the jth component. σ_z acts on $|\uparrow\rangle$ and $|\downarrow\rangle$ as $\sigma_z|\uparrow\rangle = |\uparrow\rangle$ and $\sigma_z|\downarrow\rangle = -|\downarrow\rangle$, respectively. Hence we have $\sigma_z|+\rangle = |-\rangle$, where $|-\rangle = (|\uparrow\rangle - |\downarrow\rangle)/\sqrt{2}$. Moreover,

$$L|+\rangle^{\otimes N} = \frac{\sqrt{\gamma}}{2}\sum_{j=1}^{N} |+\rangle \ldots |+\rangle|-\rangle|+\rangle \ldots |+\rangle$$

holds, where $|-\rangle$ appears in the jth component. This leads to $\langle +|^{\otimes N} L |+\rangle^{\otimes N} = 0$ and thus

$$\mathcal{E} = \left\| L|+\rangle^{\otimes N} \right\|^2 - \left| \langle +|^{\otimes N} L |+\rangle^{\otimes N} \right|^2 = \frac{\gamma N}{4}.$$

Also, we have

$$\begin{aligned} & L^\dagger L|+\rangle^{\otimes N} \\ &= \frac{\gamma}{4}\Big(N|+\rangle^{\otimes N} + 2\sum_{i\neq j} |+\rangle \ldots |-\rangle \ldots |-\rangle \ldots |+\rangle \Big), \end{aligned}$$

where $|-\rangle$ appears only in the ith and jth components ($i \neq j$). Hence,

$$\begin{aligned} \mathcal{A} &= \sqrt{2}\left(\left\| L^\dagger |+\rangle^{\otimes N} \right\|^2 + \left\| L^\dagger L |+\rangle^{\otimes N} \right\| \right) \\ &= \frac{\gamma}{4}\Big(\sqrt{2}N + \sqrt{6N^2 - 4N} \Big). \end{aligned}$$

5. GHZ state

The target is $|\mathrm{GHZ}\rangle = \big(|\uparrow\rangle^{\otimes N} + |\downarrow\rangle^{\otimes N} \big)/\sqrt{2}$. As in the previous case, the system is driven by the dephasing process $L = \sqrt{\gamma} J_z$ and an appropriate Hamiltonian H, while not subjected to MBF (i.e., $M = 0$). Using the representation (D1) we have

$$\begin{aligned} \frac{\mathcal{A}}{\sqrt{2}} &= \left\| L^\dagger |\mathrm{GHZ}\rangle \right\|^2 + \left\| L^\dagger L |\mathrm{GHZ}\rangle \right\| \\ &= \frac{\gamma}{8} N^2 \left\| |\uparrow\rangle^{\otimes N} - |\downarrow\rangle^{\otimes N} \right\|^2 + \frac{\gamma}{4\sqrt{2}} N^2 \left\| |\uparrow\rangle^{\otimes N} + |\downarrow\rangle^{\otimes N} \right\| \\ &= \frac{\gamma}{4} N^2 + \frac{\gamma}{4} N^2 = \frac{\gamma}{2} N^2, \\ \mathcal{E} &= \| L|\mathrm{GHZ}\rangle \|^2 - |\langle \mathrm{GHZ}|L|\mathrm{GHZ}\rangle|^2 \\ &= \frac{\gamma}{8} N^2 \left\| |\uparrow\rangle^{\otimes N} - |\downarrow\rangle^{\otimes N} \right\|^2 - 0 = \frac{\gamma}{4} N^2. \end{aligned}$$

6. Fock State

The target is an arbitrary Fock state $|n\rangle$ and the system operators are given by $H = i(a^\dagger - a)$, $M = \sqrt{\kappa} a^\dagger a$, and $L = \sqrt{\gamma} a$. Using $a|n\rangle = \sqrt{n}|n-1\rangle$ and $a^\dagger|n\rangle = \sqrt{n+1}|n+1\rangle$, we have

$$\begin{aligned} \mathcal{A} &= \sqrt{2}\Big(\kappa \left\| a^\dagger a |n\rangle \right\|^2 + \kappa \left\| a^\dagger a a^\dagger a |n\rangle \right\| \\ &\qquad + \gamma \left\| a^\dagger |n\rangle \right\|^2 + \gamma \left\| a^\dagger a |n\rangle \right\| \Big) \\ &= 2\sqrt{2}\kappa n^2 + \sqrt{2}\gamma(2n+1), \\ \mathcal{U} &= 2\bar{u}\sqrt{ \left\| i(a^\dagger - a)|n\rangle \right\|^2 - \langle n|i(a^\dagger - a)|n\rangle^2 } \\ &= 2\bar{u}\sqrt{2n+1}, \\ \mathcal{E} &= \kappa \left\| a^\dagger a |n\rangle \right\|^2 - \kappa \left| \langle n|a^\dagger a|n\rangle \right|^2 \\ &\qquad + \gamma \left\| a|n\rangle \right\|^2 - \gamma \left| \langle n|a|n\rangle \right|^2 \\ &= \gamma n. \end{aligned}$$

[1] W. S. Warren, H. Rabitz, and M. Dahleh, Coherent control of quantum dynamics: The dream is alive, Science **259**, 1581 (1993).

[2] L. Viola, E. Knill, and S. Lloyd, Dynamical decoupling of open quantum systems, Phys. Rev. Lett. **82**, 2417 (1999).

[3] N. Khaneja, T. Reiss, B. Luy, and S. J. Glaser, Optimal control of spin dynamics in the presence of relaxation, J. Magn. Reson. **162**, 311 (2003).

[4] D. D'Alessandro, *Introduction to Quantum Control and Dynamics* (Chapman & Hall/CRC, 2007).

[5] K. Jacobs, Engineering quantum states of a nanoresonator via a simple auxiliary system, Phys. Rev. Lett. **99**, 117203 (2007).

[6] K. Jacobs, L. Tian, and J. Finn, Engineering superposition states and tailored probes for nanoresonators via open-loop control, Phys. Rev. Lett. **102**, 057208 (2009).

[7] P. Doria, T. Calarco, and S. Montangero, Optimal control technique for many-body quantum dynamics Phys. Rev. Lett. **106**, 190501 (2011).

[8] J. Li, D. Lu, Z. Luo, R. Laflamme, X. Peng, and J. Du, Approximation of reachable set for coherently controlled open quantum systems: Application to quantum state engineering, Phys. Rev. A **94**, 012312 (2016).

[9] J. K. Stockton, R. van Handel, and H. Mabuchi, Deterministic Dicke-state preparation with continuous measurement and control, Phys. Rev. A **70**, 022106 (2004).

[10] R. van Handel, J. K. Stockton, and H. Mabuchi, Feedback contorol of quantum state reduction, IEEE Trans. Automat. Contr. **50**-6, 768/780 (2005).

[11] JM. Geremia, Deterministic and nondestructively verifiable preparation of photon number states, Phys. Rev. Lett. **97**, 073601 (2006).

[12] M. Yanagisawa, Quantum feedback control for deterministic entangled photon generation, Phys. Rev. Lett. **97**, 190201 (2006).

[13] N. Yamamoto, K. Tsumura, and S. Hara, Feedback control of quantum entanglement in a two-spin system, Automatica **43**-6, 981/992 (2007).

[14] A. Negretti, U. V. Poulsen, and K. Molmer, Quantum superposition state production by continuous observations and feedback, Phys. Rev. Lett. **99**, 223601 (2007).

[15] M. Mirrahimi and R. van Handel, Stabilizing feedback controls for quantum systems, SIAM J. Control Optim. **46**-2, 445/467 (2007).

[16] L. Bouten, R. van Handel, and M. R. James, A discrete invitation to quantum filtering and feedback control, SIAM Review **51**, 239-316 (2009).

[17] J. F. Poyatos, J. I. Cirac, and P. Zoller, Quantum reservoir engineering with laser cooled trapped ions, Phys. Rev. Lett. **77**, 4728 (1996).

[18] S. G. Schirmer and X. Wang Stabilizing open quantum systems by Markovian reservoir engineering, Phys. Rev. A **81**, 062306 (2010).

[19] N. Yamamoto, Coherent versus measurement feedback: Linear systems theory for quantum information, Phys. Rev. X **4**, 041029 (2014).

[20] M. Asjad and D. Vitali, Reservoir engineering of a mechanical resonator: generating a macroscopic superposition state and monitoring its decoherence, J. Phys. B: At. Mol. Opt. Phys. **47**, 045502 (2014).

[21] J.-R. Souquet and A. A. Clerk, Fock-state stabilization and emission in superconducting circuits using dc-biased Josephson junctions, Phys. Rev. A **93**, 060301 (2016).

[22] J. Combes, J. Kerckhoff, and M. Sarovar, The SLH framework for modeling quantum input-output networks, Advances in Physics: X **2**-3, 784/888 (2017).

[23] M. Brunelli, O. Houhou, D. W. Moore, A. Nunnenkamp, M. Paternostro, and A. Ferraro, Unconditional preparation of nonclassical states via linear-and-quadratic optomechanics, arXiv:1804.00014 (2018).

[24] C. Sayrin, et al., Real-time quantum feedback prepares and stabilizes photon number states. Nature **477**, 73 (2011).

[25] R. Vijay, et al., Stabilizing Rabi oscillations in a superconducting qubit using quantum feedback, Nature **490**, 77 (2012).

[26] D. Riste, et al., Deterministic entanglement of superconducting qubits by parity measurement and feedback, Nature **502**, 350 (2013).

[27] S. Hacohen-Gourgy, et al., Quantum dynamics of simultaneously measured non-commuting observables, Nature **538**, 491 (2016).

[28] K. C. Cox, G. P. Greve, J. M. Weiner, and J. K. Thompson, Deterministic squeezed states with collective measurements and feedback, Phys. Rev. Lett. **116**, 093602 (2016).

[29] Y. Liu, et al., Comparing and combining measurement-based and driven-dissipative entanglement stabilization, Phys. Rev. X **6**, 011022 (2016).

[30] S. Lloyd and S. Montangero, Information theoretical analysis of quantum optimal control, Phys. Rev. Lett. **113**, 010502 (2014).

[31] C. P. Koch, Controlling open quantum systems: tools, achievements, and limitations, J. Phys.: Condens. Matter **28** 213001 (2016).

[32] N. Khaneja, B. Luy, and S. J. Glaser, Boundary of quantum evolution under decoherence, PNAS **100**-23, 13162/13166 (2003).

[33] B. Qi and L. Guo, Is measurement-based feedback still better for quantum control systems?, System and Control Letters **59**-6, 333/339 (2010).

[34] B. Qi, H. Pan, and L. Guo, Further results on stabilizing control of quantum systems, IEEE Trans. Automat. Contr. **58**-5 1349/1354 (2013).

[35] C. Altafini, Controllability properties for finite dimensional quantum Markovian master equations, J. Math. Phys. **44**-6, 2357/2372 (2003).

[36] J. S. Li and N. Khaneja, Ensemble control of Bloch equations, IEEE Trans. Automat. Contr. **54**-3, 528/536 (2009).

[37] G. Dirr, U. Helmke, I. Kurniawan, and T. Schulte-Herbruggen, Lie-semigroup structures for reachability and control of open quantum systems: Kossakowski-Lindblad generators form Lie-wedge to Markovian channels, Reports Math. Phys. **64**, 93/121 (2009).

[38] I. Kurniawan, G. Dirr, and U. Helmke, Controllability aspects of quantum dynamics: A unified approach for closed and open systems, IEEE Trans. Automat. Contr. **57**-8, 1984/1996 (2012).

[39] C. O'Meara, G. Dirr, and T. Schulte-Herbruggen, Illustrating the geometry of coherently controlled unital open quantum systems, IEEE Trans. Automat. Contr. **57**-8, 2050/2056 (2012).

[40] H. Yuan, Reachable set of open quantum dynamics for a single spin in Markovian environment, Automatica **49**-4, 955/959 (2013).

[41] H. M. Wiseman and G. J. Milburn, *Quantum Measurement and Control* (Cambridge University Press, 2010).

[42] K. Jacobs, *Quantum Measurement Theory and its Applications* (Cambridge Univ. Press, 2014).

[43] H. I. Nurdin and N. Yamamoto, *Linear Dynamical Quantum Systems: Analysis, Synthesis, and Control* (Springer, 2017).

[44] M. A. Nielsen and I. L. Chuang, *Quantum Computation and Quantum information* (Cambridge University Press, 2010).

[45] R. Bianchetti, et al., Control and tomography of a three level superconducting artificial atom, Phys. Rev. Lett. **105**, 223601 (2010).

[46] L. Mandel and E. Wolf, *Optical Coherence and Quantum Optics* (Cambridge University Press, Cambridge, UK, 1997).

[47] Z. Zhang and L. M. Duan, Quantum metrology with Dicke squeezed states, New J. Phys. **16**, 103037 (2014).

[48] J. J . Bollinger, W. M. Itano, D. J. Wineland, and D. J. Heinzen, Optimal frequency measurements with maximally correlated states, Phys. Rev. A **54**, 4649 (1996).

[49] S. F. Huelga, C. Macchiavello, T. Pellizzari, A. K. Ekert, M. B. Plenio, and J. I. Cirac, Improvement of frequency standards with quantum entanglement, Phys. Rev. Lett. **79**, 3865 (1997).

[50] U. Dorner, Quantum frequency estimation with trapped ions and atoms, New J. Phys. **14**, 043011 (2012).

[51] R. P. Agarwal and D. O'Regan, *An introduction to ordinary differential equations* (Springer, 2008).